Arunansu Haldar
Satyam Suwas
Debashish Bhattacharjee
Editors

Proceedings of the International Conference on

Microstructure and Texture in Steels and Other Materials

February 5–7, 2008, Jamshedpur, India

Springer

Chapter 25
A New Flow Function to Model Texture Evolution in Symmetric and Asymmetric Rolling

Benoît Beausir and László S. Tóth

Abstract. Using a new analytic flow function, an analysis of the deformation field in symmetrical and asymmetrical rolling has been carried out. The asymmetry concerns the differences in the angular speeds of the rolling cylinders. The flow function describes the trajectory of the material flow from which the velocity field and the velocity gradient is obtained by partial derivations. The new flow function takes also into account the "discontinuity" at the entry of the material into the die. By introducing a non-homogeneous velocity distribution at the end of the flow line, the shear component in the rolling plane and in the rolling direction that is characteristic to the asymmetric rolling is naturally introduced into the deformation process. The varying velocity gradient along selected flow lines is incorporated into the viscoplastic self-consistent polycrystal plasticity model to simulate the development of the deformation texture. The effect of multiple passes as well as the asymmetries on the evolution of the deformation textures is studied for bcc iron.

25.1 Introduction

Several descriptions of the deformation by streamlines in symmetric rolling are proposed in the literature [D00, SAC07]. Most of the time they describe only the deformation zone with a discontinuity at the entry point. Concerning asymmetric rolling, the difference between the roll speeds induces a shear component in the rolling plane and in the rolling direction which is taken into account by simply adding an arbitrary chosen constant shear to get the appropriate texture evolution [JL07, LL01, LL07, ZVS03]. In this work, a new flow function is proposed; it is able to describe the discontinuity at the entry point of the plastic flow and a vary-

B. Beausir and L.S. Tóth
Laboratoire de Physique et Mécanique des Matériaux, Université de Metz, Ile du Saulcy, 57045 Metz Cedex 1, France

A. Haldar, S. Suwas, and D. Bhattacharjee (eds.), *Microstructure and Texture in Steels*,

ing shear component is naturally generated by introducing a non-uniform output velocity profile. The velocity gradient is obtained by partial derivation of the streamline function and implemented into a viscoplastic self-consistent polycrystal plasticity model to simulate the development of the deformation texture in the cases of symmetric and asymmetric rolling.

25.2 Flow Modelling

Figure 25.1 shows the geometrical parameters of the rolling process; the entry half thickness e, the half exit thickness s, the roll radius R, the angle θ corresponding to the contact zone between the sheet and the roll, the x-coordinate d of the exit flow, the top and bottom roll angular velocities ω_{roll}^{t} and ω_{roll}^{b} (rad/s), respectively, the top and bottom contact sheet velocities v_0^t and v_0^b, respectively, and the deviation part v_n of the speed at the exit of the deformation zone in the centre of the sheet. The z_s parameter defines the position of the streamline at the end of the deformation zone.

The proposed streamline is defined by:

$$\phi(x,z) = z\left[1+\left(\alpha+(1-\alpha)(x-d)^2/d^2\right)^{-n}\right]^{1/n} = z_s/\alpha, \quad \text{with } \alpha = s/e;\quad d = R\sin(\theta);\quad \cos(\theta) = (R+s-e)/R. \tag{25.1}$$

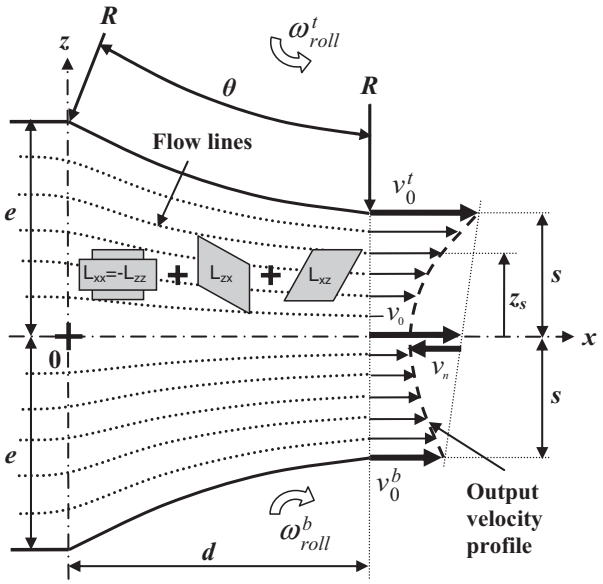

Fig. 25.1 Rolling schema.

By supposing a steady state flow, a kinematically acceptable velocity field can be defined as follows:

$$\begin{aligned} &v_x = \lambda(x,z)\partial\phi(x,z)/\partial z = \lambda(x,z)\zeta, \\ &v_z = -\lambda(x,z)\partial\phi(x,z)/\partial x = 2\lambda(x,z)z(1-\alpha)(x-d)\zeta d^{-2}\xi^{-(n+1)}\kappa^{-1}, \\ &\text{with} \quad \xi = \alpha + (1-\alpha)(x-d)^2/d^2, \quad \kappa = 1+1/\xi^n, \quad \zeta = \kappa^{1/n}. \end{aligned} \tag{25.2}$$

The function $\lambda(x,z)$ is obtained from the velocity at the exit of the deformation zone ($x=d$): $v_z|_{x=d} = 0$ and $v_x|_{x=d} = \lambda(x,z)\left(\alpha^{-n}+1\right)^{1/n}$. Then by replacing $\lambda(x,z)$ into Eq. 25.2, the velocity field is fully expressed. The output velocity distribution (at $x=d$) is supposed to be parabolic (see Fig. 25.1) and given by:

$$\begin{aligned} &v_x|_{x=d} = Az_s^2 + Bz_s + C \\ &\text{with} \quad A = v_0^t + v_0^b - 2(v_0+v_n)/2s^2; \quad B = (v_0^t - v_0^b)/2s; \quad C = v_0 + v_n. \\ &\text{and} \quad v_0^t = \omega_{roll}^t R; \quad v_0^b = \omega_{roll}^b R; \quad v_0 = R(\omega_{roll}^t + \omega_{roll}^b)/2; \quad v_n = -pv_0; \end{aligned} \tag{25.3}$$

Here p is a parameter that specifies the exact shape of the parabolic output velocity field; it can be affected by the friction conditions. Note that $v_x|_{x=d}$ is a function of z_s, thus, in order to derive the velocity gradient, the velocity field has to be fully expressed in terms of the x and z variables using the flow function before further derivation. For this purpose, we express z_s from the flow function as: $z_s = \alpha z\zeta$. Then by replacing first z_s in $v_x|_{x=d}$, the velocity gradient is finally expressed by:

$$\begin{aligned} &L_{xx} = \partial v_x/\partial x = 2\zeta(\alpha-1)(x-d)\left(3Az_s^2 + 2Bz_s + C\right)/d^2\kappa\left(\alpha^{-n}+1\right)^{1/n}\xi^{(n+1)}, \\ &L_{xz} = \partial v_x/\partial z = \alpha\zeta^2(2Az_s + B)/\left(\alpha^{-n}+1\right)^{1/n}, \\ &L_{zx} = \frac{4z_s(1-\alpha)^2(d-x)^2 v_x|_{x=d}}{\alpha d^4\kappa^2\left(\alpha^{-n}+1\right)^{1/n}} \\ &\qquad \left(\frac{(n-1)}{\xi^{2(n+1)}} + \frac{\xi^{-(n+1)}d^2\kappa}{2(1-\alpha)(d-x)^2} - \frac{z_s(2Az_s+B)}{v_x|_{x=d}\,\xi^{2(n+1)}} - \frac{\kappa(n+1)}{\xi^{(n+2)}}\right), \\ &L_{zz} = \partial v_z/\partial z = -L_{xx}, \quad L_{yy} = L_{xy} = L_{yx} = L_{yz} = L_{zy} = 0. \end{aligned} \tag{25.4}$$

This varying velocity gradient can be incorporated into the viscoplastic self-consistent polycrystal plasticity model to simulate the evolution of the deformation texture.

25.3 Velocity Field, Velocity Gradient and Texture Results

Variations of the velocity and the velocity gradient in the plastic deformation zone are first analyzed. The following combination of the parameters were chosen: $e = 2\,\text{mm}$, $s = 1\,\text{mm}$, $R = 80\,\text{mm}$, $\omega_{roll}^{t} = 1.5\ rad.s^{-1}$, $\omega_{roll}^{b} = 1.0\ rad.s^{-1}$ and $p = 0$ (that means a linear distribution of the velocity at the exit, $v_n = 0$). From Fig. 25.2 it can be seen that the discontinuity is conveniently described by the streamline function at the entry point of the flow line. The L_{zx} component of the deformation shows large variations near the entry point, at $x = 0$. The v_x component of the velocity continuously increases along the flow line (a consequence of the incompressibility condition). As the output velocity field is supposed to be linear, L_{xz} is independent of the flow lines position but varies along the x coordinate; at the exit point it can be about 4 times larger than L_{xx}.

Figure 25.3 presents the texture evolution results obtained for bcc iron for a reduction of 2 mm to 1 mm obtained in one or five passes in symmetric or asymmetric rolling (the angular velocity ratio of the rolls is 1.5) on the upper flow line (near to the faster roll) using the self consistent viscoplastic polycrystal plasticity model [MCA87]. The pencil glide mode was approached by using the $(110)<111>$ and $(112)<111>$ slip system families with equal strengths. 2000 randomly oriented grains represented the initial texture. The *n* exponent was 35. The power law of Asaro and Needleman [AN85] with a strain rate sensitivity of 0.05 was employed for the slip process.

As can be seen, the texture evolution in asymmetric rolling is very different from the symmetric rolled case. This is due to the shear component which can be about 4 times larger than the compression component. The texture in asymmetric rolling tends towards a shear type deformation texture of bcc metals, especially at increasing pass numbers.

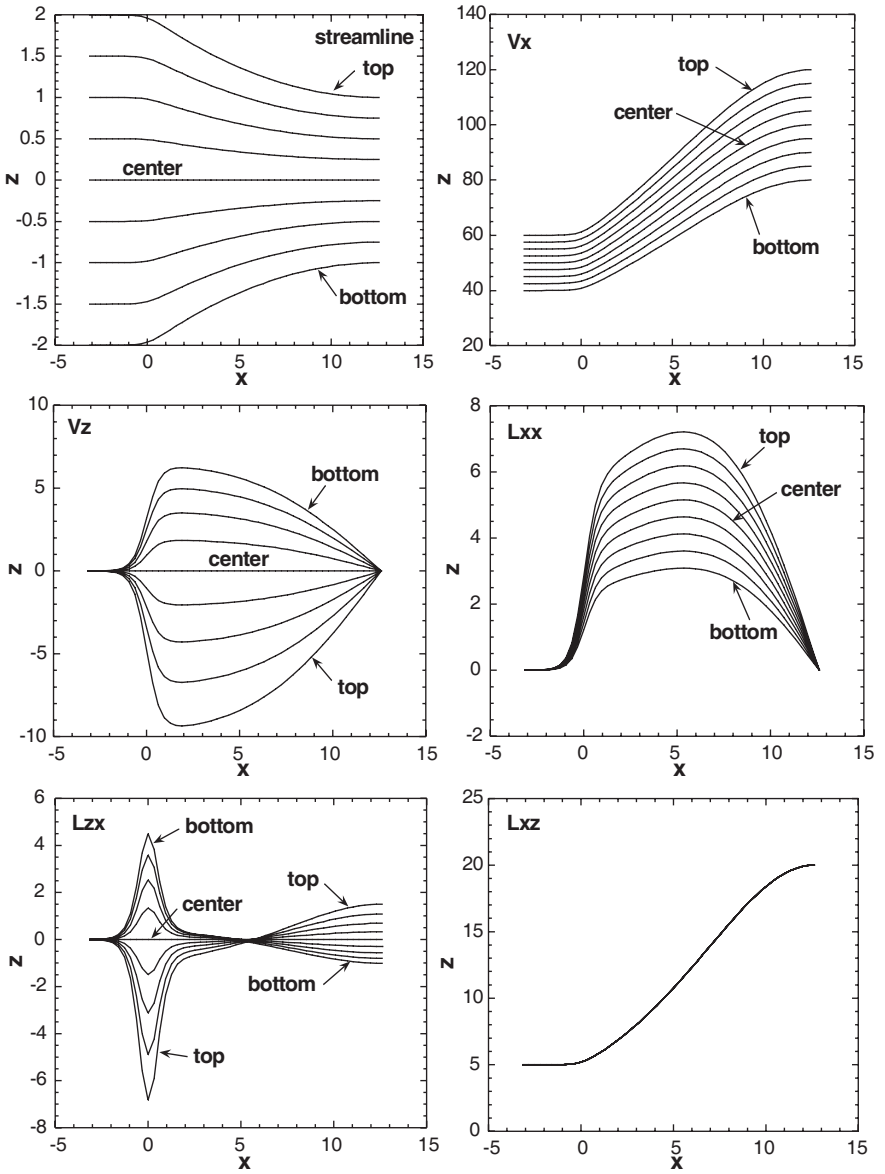

Fig. 25.2 Streamlines and values of $v_x, v_z, L_{xx}, L_{zx}, L_{xz}$ in the thickness of the sheet (along 9 lines; top, ¾, ½, ¼, centre, –¼, –½, –¾, bottom).

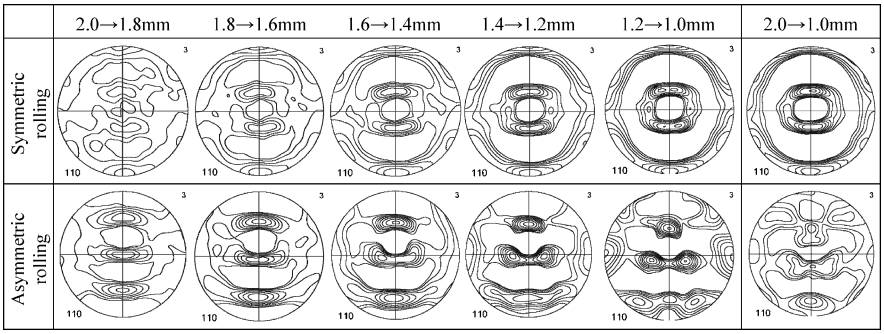

Fig. 25.3 Simulated texture evolution in Fe for symmetric and asymmetric rolling on the upper surface. ND is in the middle and RD is pointing down in all figures.

25.4 Conclusion

A new flow line function is proposed to describe symmetric or asymmetric rolling processes in multiple passes. The model predicts shear type textures in asymmetric rolling near to the surface region of the rolled plate. A comparative experimental study is needed to explore the performance of the present flow line approach.

References

[LL07] Lee JK, Lee DN, 2007. Texture control and grain refinement of AA1050 Al alloy sheets by asymmetric rolling. International Journal of Mechanical Sciences, in press

[ZVS03] Zhang F, Vincent G, Sha YH, Zuo L, Fundenberger JJ, Esling C, 2004. Experimental and simulation textures in an asymmetrically rolled zinc alloy sheet. Scripta Materialia 50, 1011–1015

[LL01] Lee SH, Lee DN, 2001. Analysis of deformation textures of asymmetrically rolled steel sheets. International Journal of Mechanical Sciences 43, 1997–2015

[JL07] Jin H, Lloyd DJ, 2007. Evolution of texture in AA6111 aluminum alloy after asymmetric rolling with various velocity ratios between top and bottom rolls. Materials Science and Engineering A 465, 267–273

[D00] Doğruoğlu AN, 2001. On constructing kinematically admissible velocity felds in cold sheet rolling. Journal of Materials Processing Technology 110, 287–299

[SAC07] Sezek S, Aksakal B, Can Y, 2007. Analysis of cold and hot plate rolling using dual stream functions. Materails and Design, in press

[AN85] Asaro RJ, Needleman A, 1985. Texture development and strain hardening in rate dependent polycrystals. Acta Metallurgica 33, 923–953

[MCA87] Molinari A, Canova G, Ahzi S, 1987. A self consistent approach of the large deformation polycrystal viscoplasticity. Acta Metallurgica 35, 2983–2994.